Spectral function and Spectral properties in a rotating QCD medium

Minghua Wei

Fudan University

November 13, 2023

Based on:
arxiv:2303.01897
Phys.Rev.D 105 (2022) 5, 054014
Chin.Phys.C 46 (2022) 2, 024102
Collaborators: Mei Huang, Yin Jiang, Chowdhury Aminul

Magnetic Field and Vorticity in Noncentral Collisions

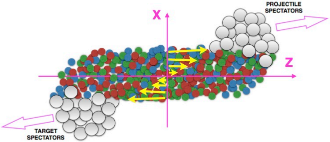

Becattini F, Karpenko I, Lisa M, et al.PRC2017

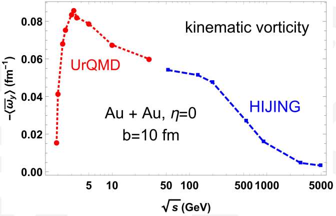

Deng W T,Huang X G,PRC2016;
Deng X G,Huang X G,Ma Y G.PRC2020

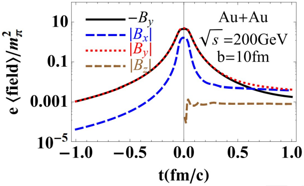

W.-T. Deng, X.-G. Huang, PRC 85, 044907 (2012)

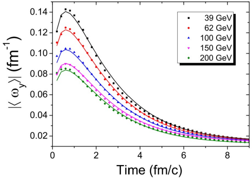

Yin Jiang, Jinfeng LiaoZiwei LinPRC2016

Geometry in rotating frame

- Metric in a co-moving frame

$$g_{\mu\nu} = \eta_{\mu\nu} + \eta_{\mu j}\delta^0_\nu v_j + \eta_{i\nu}\delta^0_\mu v_i + \eta_{ij}\delta^0_\mu\delta^0_\nu v_i v_j \qquad (1)$$

- Dirac equation in a co-moving frame

$$[i\bar{\gamma}^\mu(\partial_\mu + \Gamma_\mu) - M_f]\psi = 0. \qquad (2)$$

- Spinor connection is $\Gamma_\mu = \frac{1}{4} \times \frac{1}{2}[\gamma^a, \gamma^b]\Gamma_{ab\mu}$, and nonzero term of Spin connection is

$$\begin{aligned} \Gamma_{ij0} &= \frac{1}{2}\left(\partial_i v_j - \partial_j v_i\right), \textit{rotation} \\ \Gamma_{i0j} &= \frac{1}{2}\left(\partial_i v_j + \partial_j v_i\right), \textit{expansion, shear} \\ \Gamma_{0i0} &= -\frac{1}{2}\left(v_j \partial_i v_j + v_j \partial_j v_i\right). \end{aligned} \qquad (3)$$

- In a uniform rotating frame, i.e. $\vec{v} = \vec{\Omega} \times \vec{x}$, Spinor connection is:

$$\Gamma_{ij0} = \Omega^k \epsilon_{ijk} \quad \Gamma_0 = \frac{1}{8}\left[\gamma^i, \gamma^j\right]\Omega^k \epsilon_{ijk} \qquad (4)$$

Propagator and Self energy

- Dirac equation in a uniform rotating frame

$$[i\gamma^a\partial_a+\gamma^0\Omega\hat{J}_z - M_f]\psi = 0. \quad (5)$$

- quark propagator

$$\begin{aligned} S(\tilde{r};\tilde{r}') = & \frac{1}{(2\pi)^2}\sum_n \int \frac{dk_0}{2\pi}\int k_t dk_t \int dk_z \frac{e^{in\left(\theta-\theta'\right)}e^{-ik_0\left(t-t'\right)+ik_z\left(z-z'\right)}}{[k_0+(n+\frac{1}{2})\Omega]^2 - k_t^2 - k_z^2 - M_f^2} \\ & \times\left\{\left[[k_0+(n+\frac{1}{2})\Omega]\gamma^0 - k_z\gamma^3 + M_f\right]\right. \\ & \times\left[J_n(k_t r)J_n(k_t r')\mathcal{P}_+ + e^{i(\theta-\theta')}J_{n+1}(k_t r)J_{n+1}(k_t r')\mathcal{P}_-\right] \\ & \left. - i\,\gamma^1 k_t e^{i\theta}J_{n+1}(k_t r)J_n(k_t r')\mathcal{P}_+ - \gamma^2 k_t e^{-i\theta'}J_n(k_t r)J_{n+1}(k_t r')\mathcal{P}_-\right\}, \end{aligned} \quad (6)$$

- One-loop Polarization function

$$\Pi^{ab}(q) = -iN_f N_c\int d^4\tilde{r}\,\mathrm{Tr}_D[i\gamma^a S(0;\tilde{r})i\gamma^b S(\tilde{r};0)]e^{iq\cdot\tilde{r}}, \quad (7)$$

Dilepton Rate in QGP

- Dilepton in HIC

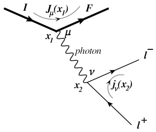

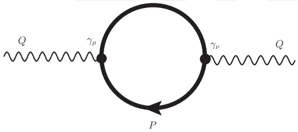

- The dilepton rate is related to the Lepton tensor and the photon tensor:

$$dR_{l\bar{l}} = 2\pi e^2 e^{-\beta\omega} L_{\mu\nu}(p_1, p_2)\rho^{\mu\nu}(\omega, \mathbf{q}) \frac{d^3\mathbf{p}_1}{(2\pi)^3 E_1} \frac{d^3\mathbf{p}_2}{(2\pi)^3 E_2} \tag{8}$$

- Combined with Lepton tensor for plane wave

$$\frac{dR_{l\bar{l}}}{d^4q} = \frac{\alpha}{12\pi^4} \frac{n_B(\omega)}{q^2} \left(1 + \frac{2m_l^2}{q^2}\right)\left(1 - \frac{4m_l^2}{q^2}\right)^{1/2} \mathrm{Im}\left[\Pi^\mu_\mu(\omega, \mathbf{k})\right]. \tag{9}$$

Scenarios for Dilepton production in QGP

- Lepton pairs not affected by the medium

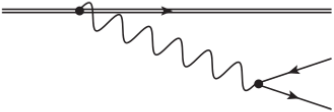

$$L^{\mu\nu} = 2\left(-q^2 g^{\mu\nu} + q^\mu q^\nu - k^\mu k^\nu\right) \tag{10}$$

- Lepton pairs affected by rotating medium or EM field.

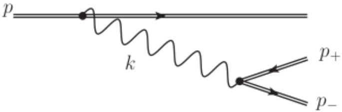

- Lepton states in the rotating medium $|\, p_t, p_z, n, s\rangle \longrightarrow$ states in the detectors $|\, p, s\rangle$

Spectral function in a rotating QCD medium

- Spectral function is related to the imaginary part of the vector current-current correlation function at one-loop level:

$$\sigma_V(q) = \frac{1}{\pi}\mathrm{Im}\Pi^a_a(q), \tag{11}$$

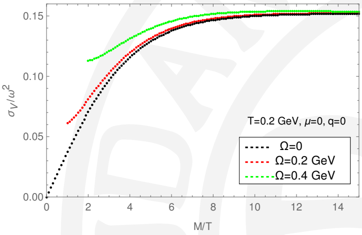

Figure 1: Spectral function as a function of temperature scaled invariant mass for different values of rotation.

Spectral function in a rotating QCD medium

- Spectral function is related to the imaginary part of the vector current-current correlation function at one-loop level:

$$\sigma_V(q) = \frac{1}{\pi}\mathrm{Im}\Pi^a_a(q), \tag{12}$$

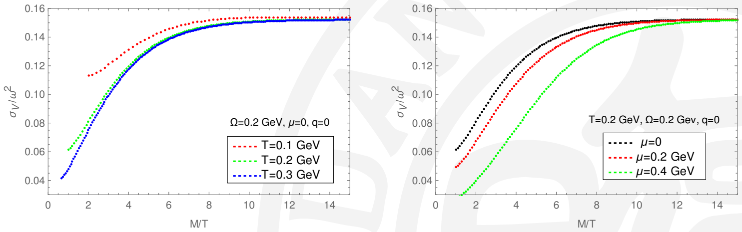

Figure 2: Left panel: SF as a function of temperature scaled invariant mass for different values of temperature; Right panel: SF for different values of chemical potential.

Dilepton Rate Enhancement under Rotation

- Dilepton rate expression:

$$\frac{dR_{l\bar{l}}}{d^4q} = \frac{\alpha}{12\pi^4}\frac{n_B(\omega)}{M^2}\,\mathrm{Im}\left[\Pi^a_a(\omega,|\mathbf{q}|,q_z)\right], \tag{13}$$

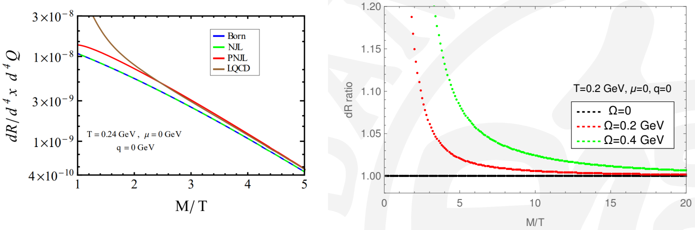

Figure 3: Dilepton rate as a function of invariant mass with different angular velocities.

q dependence for $\mathrm{Im}\Pi^{ab}$

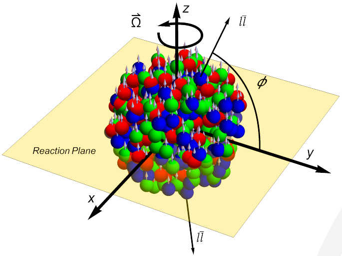

Figure 4: A sketch map for dilepton emissions from rotating QGP.

- Explicit form of $\mathrm{Im}\Pi^{ab}$:

$$\begin{aligned}
&\mathrm{Im}[\Pi^{11}(\omega,\vec{q})+\Pi^{22}(\omega,\vec{q})] \\
&=-\frac{1}{2}\pi N_f N_c \sum_{\eta=\pm1}\int_{p_-^\Omega}^{p_+^\Omega}\frac{pdp}{(2\pi)^2}\cdot\frac{1}{|\vec{q}|E_p} \\
&\times\Big\{2E_p(\omega-E_p+\eta\Omega)+[(3\frac{q_z^2}{q^2}-1)(p\cos\theta_1)^2 \\
&+p^2(1-\frac{q_z^2}{q^2})+2\frac{q_z^2}{q}p\cos\theta_1]+2M_f^2\Big\} \\
&\times[1-f(E_p-\mu-\frac{\eta\Omega}{2})-f(E_p+\mu-\frac{\eta\Omega}{2})].
\end{aligned} \tag{14}$$

Constrain the integral region and the angle between $\vec{p}$ and $\vec{q}$:

$$p_\pm^\Omega=\pm\frac{|\vec{q}|}{2}+\frac{\omega+\eta\Omega}{2}\sqrt{1-\frac{4M_f^2}{(\omega+\eta\Omega)^2-\vec{q}^2}} \quad \cos\theta_1=\frac{(\omega+\eta\Omega)^2-2(\omega+\eta\Omega)\sqrt{p^2+M_f^2}-q^2}{2pq} \tag{15}$$

ϕ dependence for $\mathrm{Im}\Pi^{ab}$

- Elliptic flow coefficient v_2 is calculated in mid-rapidity, i.e. $q_x = 0$ and $\frac{q_z}{q_T} = \sin\phi$. One can extract ϕ dependent part of $\mathrm{Im}\Pi^{ab}$:

$$
\begin{aligned}
&(\mathrm{Im}[\Pi^{11}(\omega,\vec{q}) + \Pi^{22}(\omega,\vec{q})])_{dep} \\
&= -\frac{1}{2}\pi N_f N_c \cos 2\phi \sum_{\eta=\pm1}\int_{p_-^\Omega}^{p_+^\Omega}\frac{pdp}{(2\pi)^2}\frac{-\frac{3}{2}(p\cos\theta_1)^2 + \frac{p^2}{2} - pq\cos\theta_1}{qE_p} \\
&\quad\times [1 - f(E_p - \mu - \frac{\eta\Omega}{2}) - f(E_p + \mu - \frac{\eta\Omega}{2})]\Big\}\ ,
\end{aligned}
\tag{16}
$$

$$
\begin{aligned}
\mathrm{Im}\Pi^{33}(\omega,\vec{q})_{dep} &= -\frac{1}{2}\pi N_f N_c \cos 2\phi \sum_{\eta=\pm1}\int_{p_-}^{p_+}\frac{pdp}{(2\pi)^2}\Big\{\frac{[\frac{3}{2}(p\cos\theta_0)^2 - \frac{1}{2}p^2 + pq\cos\theta_0]}{qE_p} \\
&\quad\times [1 - f(E_p - \mu - \frac{\eta\Omega}{2}) - f(E_p + \mu - \frac{\eta\Omega}{2})]\Big\}\ .
\end{aligned}
\tag{17}
$$

Ellipticity of Dilepton Production under Rotation

- Angular dependence of dilepton production rate in the transverse plane.

$$E\frac{\mathrm{d}^3R}{\mathrm{d}^3\mathbf{q}} = \frac{1}{2\pi}\frac{\mathrm{d}^2R}{q_T\ \mathrm{d}q_T\ \mathrm{d}y}\left(1+2\sum_{n=1}^{\infty}v_n\cos\left[n\left(\phi-\Psi_{\mathrm{RP}}\right)\right]\right), \qquad (18)$$

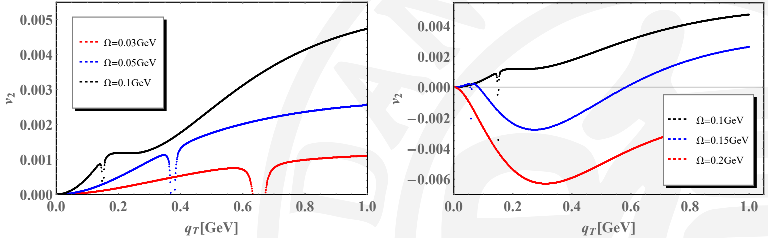

Figure 5: Elliptic flow v_2 as a function of q_T with T=160 MeV,M=200MeV and different angular velocities Ω =0.03,0.05,0.1,0.15,0.2 GeV.

Invariant mass dependence of elliptic flow v_2

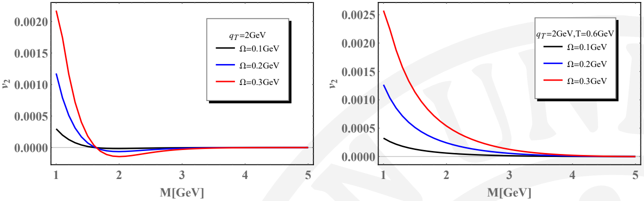

Figure 6: Elliptic flow v_2 at T=160 MeV(left) and 600 MeV(right).

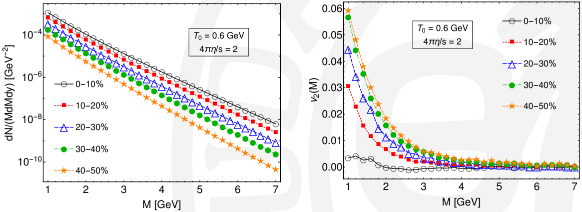

Figure 7: Dilepton production and elliptic flow from an anisotropic QGP (Babak S. Kasmaei and Michael Strickland, PRD2019)

Related works by other people

- Quark propagator and di-lepton production rate in a hot, dense and very strongly magnetized rotating Quark-Gluon Plasma[Aritra Das, arxiv:2310.11869]
- Bulk viscosity of rotating, hot and dense spin 1/2 fermionic systems from correlation functions

$$\Pi_\zeta(q) = i\int d^4 r e^{iq\cdot r}\left\langle \mathcal{P}^*(r)\mathcal{P}^*(0)\right\rangle_R \tag{19}$$

[Sarthak Satapathy, arxiv:2307.09953]

- Electromagnetic radiation at extreme angular velocity

$$S_{fi} = -ie\int dt\int d\phi\int dz\boldsymbol{j}_{fi}(t,\phi,z)\cdot\boldsymbol{A}^*(t,\phi,z,R) \tag{20}$$

[Matteo Buzzegoli and Kirill Tuchin,arxiv:2308.10349]

Methods for QCD Phase diagram under rotation

- NJL model with spinor connection[arxiv:1606.03808]

$$\mathcal{L} = \bar{\psi}\left[i\bar{\gamma}^{\mu}\left(\partial_{\mu}+\Gamma_{\mu}\right)-m\right]\psi + G_S\left[(\bar{\psi}\psi)^2+\left(\bar{\psi}i\gamma_5\vec{\tau}\psi\right)^2\right] \tag{21}$$

- 3-flavor NJL model with spinor connection

$$\begin{aligned}\mathcal{L}_{\mathrm{3NJL}} =& \bar{\psi}[i\bar{\gamma}^{\mu}(\partial_{\mu}+\Gamma_{\mu})-m_f]\psi \\ &+ G_S\sum_{a=0}^{8}\left[\left(\bar{\psi}\lambda^a\psi\right)^2+\left(\bar{\psi}i\gamma_5\lambda^a\psi\right)^2\right] \\ &- G_V\sum_{a=0}^{8}\left[\left(\bar{\psi}\gamma_{\mu}\lambda^a\psi\right)^2+\left(\bar{\psi}i\gamma_{\mu}\gamma_5\lambda^a\psi\right)^2\right] \\ &- K\left[\det\bar{\psi}\left(1+\gamma_5\right)\psi+\det\bar{\psi}\left(1-\gamma_5\right)\psi\right],\end{aligned} \tag{22}$$

QCD Phase diagram

- Grand potential

$$\Omega_f(r) = \frac{N_c}{8\pi^2} T \sum_n \int dk_t^2 \int dk_z \left[J_n(k_t r)^2 + J_{n+1}(k_t r)^2 \right] \times \left[E_k/T + \ln\left(1 + e^{-(E_k - (n+\frac{1}{2})\Omega)/T}\right) + \ln\left(1 + e^{-(E_k + (n+\frac{1}{2})\Omega)/T}\right) \right]. \tag{23}$$

$$\Omega_{\text{tot}}(r) = \sum_{f=u,d,s} \left(2G_S\sigma_f^2 - \Omega_f\right) + 4K\sigma_u\sigma_d\sigma_s. \tag{24}$$

- Gap equations and dynamical quark masses

$$\frac{\partial\Omega_{\text{tot}}}{\partial\sigma_f} = 0, \quad \frac{\partial^2\Omega_{\text{tot}}}{\partial\sigma_f^2} > 0. \tag{25}$$

$$M_f \equiv m_f - 4G_S\sigma_f + 2K \prod_{f'\neq f} \sigma_{f'}. \tag{26}$$

Chiral condensates and dynamical quark masses

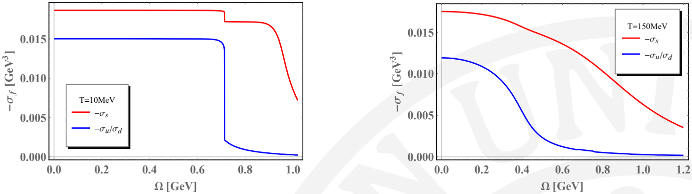

Figure 8: Chiral condensates as functions of angular velocity.

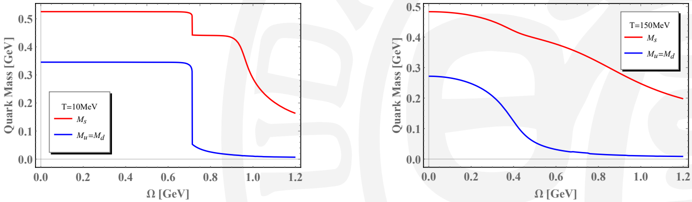

Figure 9: Dynamical quark masses as functions of angular velocity.

Random Phase Approximation

- RPA

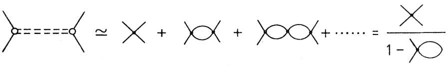

- Pole mass

$$D_\sigma(q^2) = \frac{2G_S}{1 - 2G_S \Pi_s(q^2)}, \tag{27}$$

- Polarization function

$$\Pi_s(q) = -i \int d^4\tilde{r}\, Tr_{sfc}[iS(0;\tilde{r})iS(\tilde{r};0)]e^{iq\cdot\tilde{r}}, \tag{28}$$

- Quark propagator

$$\begin{aligned} S(\tilde{r};\tilde{r}') = & \frac{1}{(2\pi)^2}\sum_n \int \frac{dk_0}{2\pi} \int k_t dk_t \int dk_z \frac{e^{in\left(\theta-\theta'\right)} e^{-ik_0\left(t-t'\right)+ik_z\left(z-z'\right)}}{[k_0+(n+\frac{1}{2})\Omega]^2 - k_t^2 - k_z^2 - M_f^2} \\ & \times \left\{ \left[[k_0+(n+\frac{1}{2})\Omega + \mu]\gamma^0 - k_z\gamma^3 + M_f \right] \right. \\ & \times \left[J_n(k_t r)J_n(k_t r')\mathcal{P}_+ + e^{i(\theta-\theta')}J_{n+1}(k_t r)J_{n+1}(k_t r')\mathcal{P}_- \right] \\ & \left. - i\,\gamma^1 k_t e^{i\theta} J_{n+1}(k_t r)J_n(k_t r')\mathcal{P}_+ - \gamma^2 k_t e^{-i\theta'} J_n(k_t r)J_{n+1}(k_t r')\mathcal{P}_- \right\}, \end{aligned} \tag{29}$$

Scalar Meson Mass

- Scalar Meson Mass at T=150 MeV , μ=100MeV, and μ=200MeV

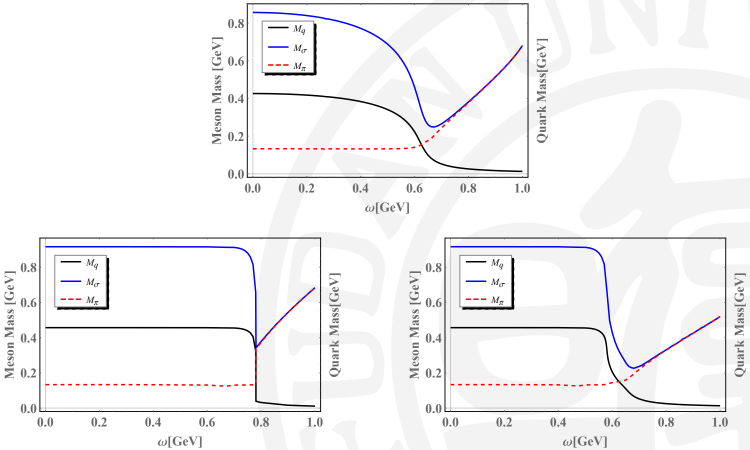

Vector Meson Mass

- Polarization function

$$\Pi^{\mu\nu,ab}(q) = -i\int d^4\tilde{r}\, Tr_{sfc}[i\gamma^\mu\tau^a S(0;\tilde{r})i\gamma^\nu\tau^b S(\tilde{r};0)]e^{iq\cdot\tilde{r}}. \tag{30}$$

- Propagator can be decomposed into three spin states

$$\Pi^{\mu\nu}_\rho = A_1^2 P_1^{\mu\nu} + A_2^2 P_2^{\mu\nu} + A_3^2 L^{\mu\nu} + A_4^2 u^\mu u^\nu, \tag{31}$$

$$D^{\mu\nu}_\rho(q^2) = D_1(q^2)P_1^{\mu\nu} + D_2(q^2)P_2^{\mu\nu} + D_3(q^2)L^{\mu\nu} + D_4(q^2)u^\mu u^\nu, \tag{32}$$

- Pole mass

$$D_i(q^2) = \frac{4G_V}{1+4G_V A_i^2}, \quad 1+4G_V A_i^2 = 0 \tag{33}$$

Spin Alignment with Thermal Equilibrium

- Meson spectral function[arxiv:2209.01872]

$$\xi_\lambda(k) \equiv \frac{1}{\pi}\,\mathrm{Im}\,D_\lambda(k) = \frac{(4G_V)^2\,\mathrm{Im}\,A_\lambda(k)}{\pi\left\{[1+4G_V\,\mathrm{Re}\,A_\lambda(k)]^2+[4G_V\,\mathrm{Im}\,A_\lambda(k)]^2\right\}} \tag{34}$$

- Assuming thermal equilibrium, particle number density for

$$f_\lambda = \frac{1}{\exp\left(M_\lambda/T\right)-1} + \int d\omega\,\frac{2\omega\xi_\lambda^*(\omega)}{\exp(\omega/T)-1} \tag{35}$$

- Spin alignment

$$\rho_{00} \equiv \frac{f_0}{\sum_{\lambda=0,\pm1} f_\lambda} \tag{36}$$

Spectral functions for Vector Meson ϕ

- The spectral function is shifted to the left/right side.

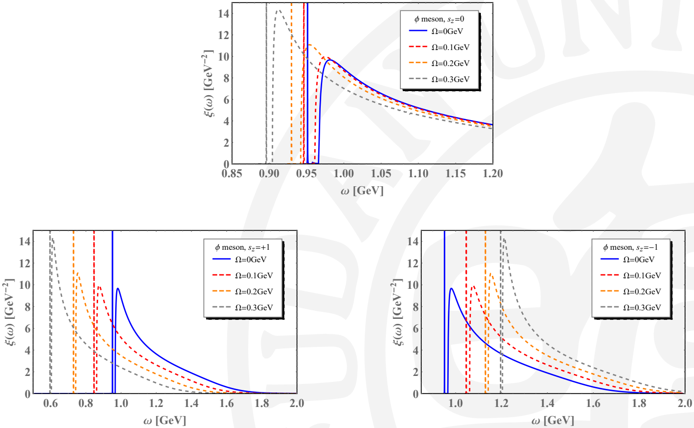

Spectral functions for Vector Meson ρ

- For ρ mesons at the temperature $T = 150$ MeV, spectral functions only have continuum parts and appear as single peaks.

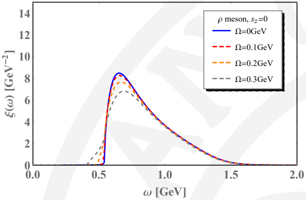

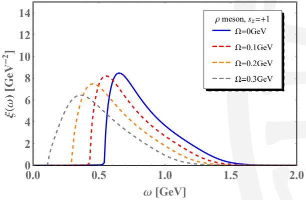

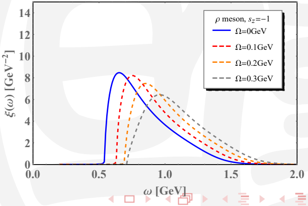

Spin alignment for Vector Meson ϕ

- Spin alignment for Vector Meson ϕ and ρ in 150 MeV

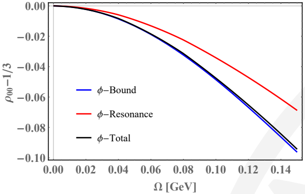

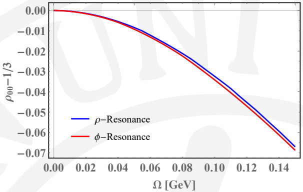

- Comparison with leading order of quark coalescence model[arxiv:1711.06008]

$$\rho_{00}^{\phi,coal} = \frac{1}{3} - \frac{1}{9}(\beta\Omega)^2 \tag{37}$$

$$\rho_{00}^{\phi}(\Omega) = \frac{1}{3} - 5.10\Omega^2 + 39.62\Omega^4, \tag{38}$$

1. Introduction
2. Thermal dilepton rate and its ellipticity
3. Meson Spectra and Spin Alignment
4. **Summary and Outlook**
5. Appendix

Summary and Outlook

- In a rotating medium, the dilepton rate is enhanced;
- Azimuthal anisotropy of the dilepton production is induced by rotation;
- $\rho_{00} - 1/3$ is negative in the rotating medium. Compared with the quark coalescence model, results from NJL model don't have remarkable improvement currently.
- cold vacuum doesn't rotate: $|\,0\rangle_{rotating} = |\,0\rangle_{no-rotating}$, How about $|\,\Omega\rangle_{rotating}$ and $|\,\Omega\rangle_{no-rotating}$? Perturbative study is important(*But hard*)!
- Other hydrodynamic gradients(vorticity, expansion, shear tensor) should take into account(see Feng Li,Shuai Liu, 2206.11890).

Thanks for your attention!

An optional profile

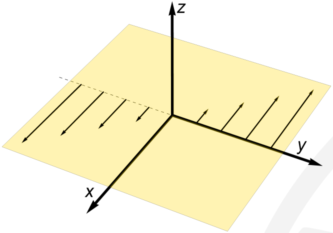

$$v_1 = v_x = -\Omega y \qquad v_2 = v_y = 0 \tag{39}$$

$$\begin{aligned}
\Gamma_{120} &= \frac{1}{2}(\partial_x v_y - \partial_y v_x) = \frac{1}{2}\Omega \\
\Gamma_{102} &= -\frac{1}{2}\Omega \quad \Gamma_{201} = -\frac{1}{2}\Omega \\
\Gamma_{010} &= \frac{1}{2}(v_j \partial_x v_j + v_j \partial_j v_x) = \frac{1}{2} v_y \cdot \Omega = 0 \\
\Gamma_{020} &= \frac{1}{2}(v_j \partial_y v_j + v_j \partial_j v_y) = \frac{1}{2} v_x \Omega = -\frac{1}{2} y \Omega^2
\end{aligned} \tag{40}$$

FAQ

- singularities show up in v_2 as a function of q_T. These singularities emerge from a 4-momentum non-conservation in the rotating frame, because δ function in the imaginary part has been modified by $\delta(\omega - E_p - E_k + \eta\Omega)$ As a consequence, $p_{\pm}^{\Omega}$ will reach an extremely large value to satisfy $\omega - E_p - E_k + \eta\Omega = 0$. We have shown that the rotation effect had modified the domain of integration by $p_{\pm}^{\Omega} = \pm\frac{q}{2} + \frac{\omega+\eta\Omega}{2}\sqrt{1 - \frac{4M_f^2}{(\omega+\eta\Omega)^2 - q^2}}$. Resonance is generated at $q_t = \omega + \eta\Omega$, and the singularity will show up with uniform rotation, which is similar to the forced oscillator without damping.

Components for $\mathrm{Im}\Pi^{ab}$

$$
\begin{aligned}
&\mathrm{Im}[\Pi^{11}(\omega,\vec{q})+\Pi^{22}(\omega,\vec{q})] \\
&= -\frac{1}{2}\pi N_f N_c \sum_{\eta=\pm 1}\int_{p_-^\Omega}^{p_+^\Omega}\frac{pdp}{(2\pi)^2}\cdot\frac{1}{|\vec{q}|E_p} \\
&\times\Big\{2E_p(\omega-E_p+\eta\Omega)+[(3\frac{q_z^2}{q^2}-1)(p\cos\theta_1)^2 \\
&+p^2(1-\frac{q_z^2}{q^2})+2\frac{q_z^2}{q}p\cos\theta_1]+2M_f^2\Big\} \\
&\times[1-f(E_p-\mu-\frac{\eta\Omega}{2})-f(E_p+\mu-\frac{\eta\Omega}{2})].
\end{aligned}
\tag{41}
$$

$$
p_\pm^\Omega=\pm\frac{|\vec{q}|}{2}+\frac{\omega+\eta\Omega}{2}\sqrt{1-\frac{4M_f^2}{(\omega+\eta\Omega)^2-\vec{q}^2}} \tag{42}
$$

Expansion

$$\frac{1/(\mathrm{Exp}[(M)/T]-1)}{1/(\mathrm{Exp}[(M+\Omega)/T]-1)+1/(\mathrm{Exp}[(M)/T]-1)+1/(\mathrm{Exp}[(M-\Omega)/T]} \tag{43}$$

The result is:

$$\rho_{00}^{\phi}=\frac{1}{3}-\frac{\left(e^{M/T}\left(1+e^{M/T}\right)\right)\Omega^2}{9\left(\left(-1+e^{M/T}\right)^2T^2\right)}+\frac{e^{M/T}\left(-1-7e^{M/T}-3e^{\frac{2M}{T}}+3e^{\frac{3M}{T}}\right)}{108\left(-1+e^{M/T}\right)^4T^4} \tag{44}$$